

Practical Implementation of Ultrawideband Partial Discharge Detectors

G. C. Stone¹ H. G. Sedding,, N. Fujimoto, and J. M Braun
Ontario Hydro, Toronto, Canada

IEEE Transactions on Electrical Insulation Vol. 27 No. 1, February 1992

ABSTRACT

Since the introduction of partial discharge (PD) testing four decades ago, the majority of conventional electrical measurements of PD is performed with detectors operating in the 10 kHz to 1 MHz range. In the past decade, advances in electronic instrumentation have permitted the measurement of PD with bandwidths up to 1 GHz. Since PD pulses are fundamentally events with durations as low as a few ns, PD measurements with such ultrawideband (UWB) detection methods can provide several benefits in certain situations. In particular, UWB detection can improve the fundamental signal-to-noise ratio, permitting reliable PD detection at 0.01 pC. Additionally, using the properties of electromagnetic wave propagation associated with ns duration current pulses, methods to eliminate external noise on a pulse-by-pulse basis can be implemented with UWB detection. Finally, UWB detection of the PD current pulse can lead to greater fundamental understanding of the physical processes of PD in solid dielectrics. UWB detection has had an important impact on PD measurements in gas-insulated switchgear insulating spacers and on-line generator stator winding PD tests. Examples of the application of UWB detection systems to these areas are presented.

1. INTRODUCTION

Partial Discharge (PD) tests are widely employed as quality control and diagnostic tests to determine the fitness for use of V equipment employing solid electrical insulation [1]. The standard PD detection method presently used by industry has remained virtually unchanged in its essential aspects for over three decades. Partial discharges are normally detected as current pulses by a coupling capacitor in parallel, or by a suitable impedance in series, with the test piece. The signals from the coupling impedance are filtered to remove any power frequency components. The characteristics of the filter, which should also include consideration of other system components such as amplifiers, are such that the current pulse signals are integrated to yield a pulse magnitude which is proportional to the charge in the PD pulse [1,2]. For all conventional PD detectors presently commercially available, the filters have a bandwidth ranging from ~ 30 kHz (narrow band) to ~ 500 kHz (wideband), at center frequencies of ~ 10 kHz to ~ 2

MHz. The integrated pulses are normally displayed on an oscilloscope, so that the magnitude and phase position of the PD pulses can be displayed vs. the ac voltage.

During the past decade, the availability of fast analog-to-digital converters has made practical the digital storage and

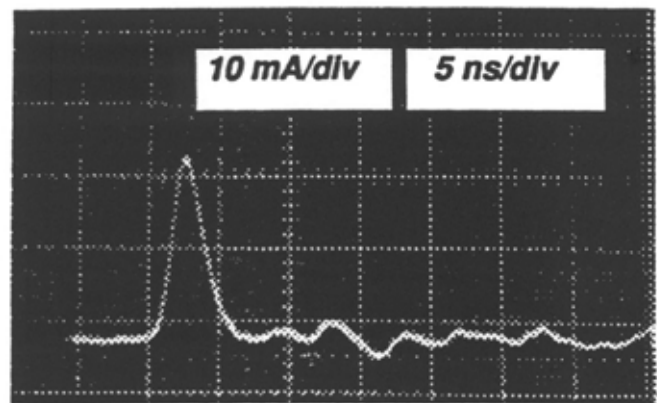


Figure 1.

Example of fast PD pulse shape as measured on a laboratory sample with a single void in unfilled epoxy. Pulses of this type usually have ns to sub-ns risetimes and durations of a few ns. The measurement was made with an oscilloscope with an analog bandwidth of 1000 MHz.

analysis of PD signals from conventional detectors. This in turn has led to the easy implementation of pulse height analysis and pulse phase analysis which was pioneered, with considerable difficulty, two decades ago by Bartnikas [3] and Kelen [4]. Similarly, advances in computer hardware and the recent introduction of powerful software aids have permitted digitized PD data to be easily manipulated and displayed, including three-dimensional plots. More than a dozen organizations have now produced post-detection processing packages to analyze PD data, including plots of pulse magnitude vs. ac phase position vs. pulse repetition rate [5-12].

One advantage of these recent developments is that the PD data are permanently stored and available for off-line analysis (and re-analysis). Inspection of the PD data by other experts is thus possible beyond the person doing the actual test. In addition, common software graphical tools permit extraction of more detail from the PD data, »such as

information on possible causes of the PD (from polarity, magnitude and phase characteristics), and the more certain discrimination of electrical noise from PD through the use of pulse height and pulse phase analysis [13,14]. Prior to the introduction of sophisticated post-detection processing techniques, PD source identification and extraction of PD from noise were only performed with some success by a few highly skilled specialists, subjectively observing PD behavior on an oscilloscope. Digital acquisition also permits statistical analysis of the raw PD data, or the calculation of various summary components such as standard deviation, skewness, etc. to describe the pulse height and pulse phase PD plots [15].

Although digital post-detection processing of data from conventional PD detectors allows a larger group of people to extract meaningful data from PD tests, even greater gains can be made if the PD detectors themselves are improved. In particular, PD measuring systems which have an ultrawide bandwidth (UWB) of ~ 500 MHz (rather than ~ 200 kHz of conventional detectors) can result in three distinct advantages [16], as discussed extensively in this paper. The first is that there is often greater sensitivity to PD if the PD is detected with an ultrawide bandwidth. In addition UWB PD detection can facilitate elimination of external interference. Finally, with suitable UWB detectors, the true shape of the PD current pulses can be detected, providing another means of ascertaining the nature and source of the PD in the insulation system. These improvements require PD detectors significantly different from the detectors traditionally used by industry, since they operate at frequencies ~ 300 MHz.

This paper describes new practical PD detection methods for rotating machine and gas-insulated switchgear (GIS) applications which rely on UWB PD detection. In the GIS application, the UWB system permits detection of PD in insulating spacers down to the 0.01 pC level under factory-like acceptance testing at voltages ~ 400 kV.

This compares to the normal sensitivity of 5 pC in similar situations. The rotating machine applications show how UWB detection permits reliable extraction of PD from signals which contain external noise as much as 1000 x larger than the PD signals. The post-detection digital capture and analysis of the PD pulses described above can still be performed on the data from UWB detectors to enhance the analysis further. Prior to describing the applications, a review of the benefits of UWB PD detection is presented.

With UWB PD detection, the current component of the PD pulse is measured, as compared to charge in conventional detection systems. Due to the very fast nature of PD pulses, detection of these currents with UWB techniques results in three advantages.

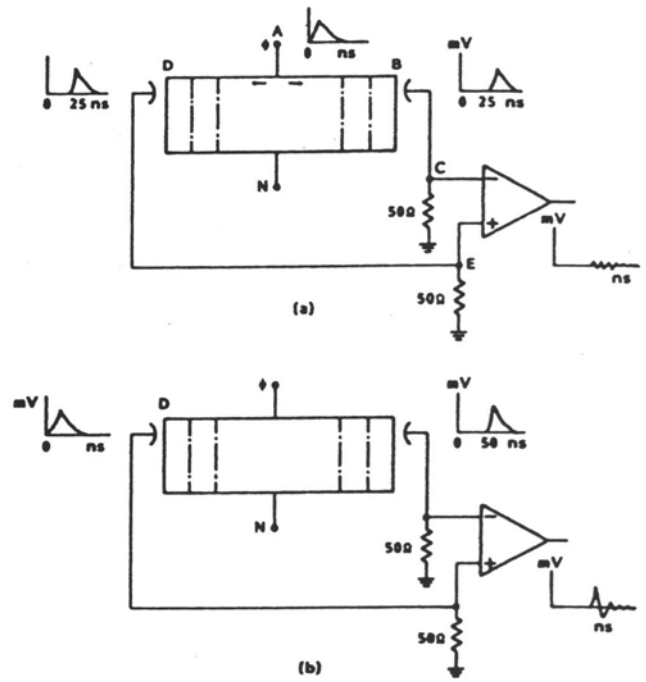


Figure 2.

Rejection of common-mode electrical noise while maintaining sensitivity to winding discharges is obtained by electrically balancing the coaxial cables connecting the couplers to the external differential amplifier. The electrical length ABC must equal ADE. In (a), a noise pulse from the power system arrives simultaneously at the inputs of the differential amplifier, resulting in no output. In (b) a discharge pulse (near D) yields a nonzero output because the electrical signal arrives at the positive input of the differential amplifier before it arrives at the negative input.

2. ULTRAWIDEBAND PARTIAL DISCHARGE DETECTION

2.1 INCREASED SENSITIVITY

The underlying physical processes which give rise to PD are very short lived [17]. PD pulse currents have been measured to have risetimes between 350 ps and ~ 3 ns, and pulse durations of ~ 1 to ~ 5 ns [17,18]. Such fast current pulses have been measured in voids (see Figure 1), from small ‘floating’ metal particles such as those found in GIS, as well as from electrical tree growth [18]. Although longer duration pulses are possible, many PD pulses in practical equipment will have a true pulse duration of only ~ 3 ns. Such short pulses have an equivalent (Fourier) bandwidth of ~ 200 MHz. For example, a 350 ps risetime corresponds to 1 GHz in the frequency domain. Thus it is clear that PD pulses result in harmonic components up to ~ 1 GHz.

Conventional detectors, limited to the low MHz range, do not respond to much of the energy in the PD pulse.

Elementary information theory indicates that the detected energy from a PD pulse will increase almost linearly with bandwidth, up to ~ 200 MHz (assuming ns duration PD pulses)

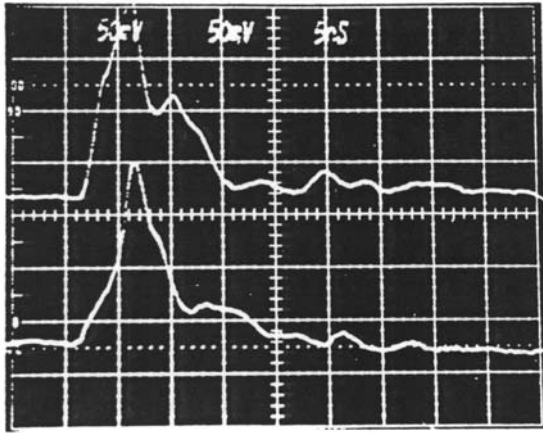


Figure 3.

Example of SSC response to PD pulses occurring on an operating 22 kV, 500 MW turbine generator. Gain = 50 mV/div, timebase = 5 ns/div.

[16]. In situations where there is little external electrical interference, typically in measurements from bridge-type detectors or unshielded rooms, the principal limitation to PD sensitivity is caused by thermal noise in amplifiers and resistors [16]. However, the energy in such 'white' noise only increases as the square root of the detection bandwidth. Comparison of the increase in detected PD energy and thermal noise energy, as a function of bandwidth, indicates that the PD signal to amplifier noise ratio improves as the detection bandwidth increases [16]. In particular, for a 1.5 ns full width at half maximum (FWHM) PD pulse, the PD sensitivity at 1 MHz bandwidth is ~ 0.1 pC, compared to 0.01 pC at 350 MHz (Figure 7 in [16]). Comparative measurements were performed with a commercially available PD detector and a system comprised of an in-line resistor connected to a 900 MHz bandwidth oscilloscope (Tektronix 7104). Apart from the detectors, all other experimental conditions were the same, i.e., test object, power supply, etc. The limit of sensitivity for the conventional detector was found to be 0.4 pC, whereas for the UWB technique the lower limit was 0.04 pC. Thus the UWB technique produced an order of magnitude improvement in sensitivity. Hence UWB PD detection will greatly increase the sensitivity to PD if the electrical noise is only due to electronic sources. An example of the practical improvement in PD detection sensitivity in GIS is described below.

2.2 REDUCTION IN EXTERNAL INTERFERENCE

When PD tests are done in the field, for example in substations or generating stations, external electrical interference is usually the predominant source of noise. Thus the actual PD sensitivity depends on the magnitude of this noise. External noise sources include corona or PD from the HV supply, discharges from floating components in a high electric field, sparking from poor electrical contacts, thyristor switching interference, and arcing from slip ring brushes or arc welders. All these noise sources can produce current pulses which

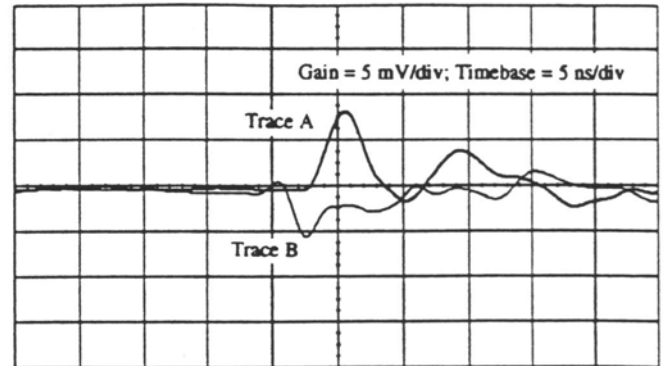


Figure 4.

SSC response to a PD pulse obtained from an operating 22 kV, 500 MW turbine generator. Trace A is the output of the SSC closest to the slip ring end of the generator. Trace B is from the output on the SSC which is further into the slot. In this case the PD pulse is propagating outward from the slot portion of the stator, i.e. B triggers before A.

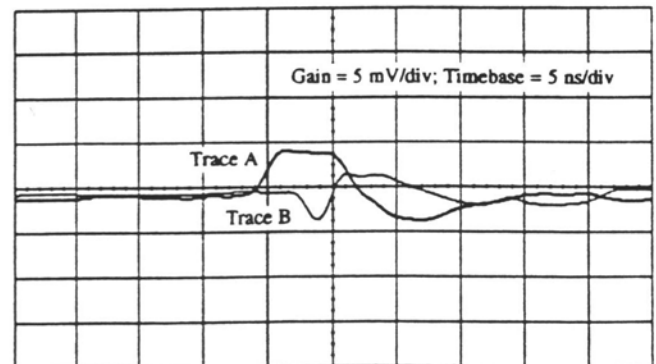


Figure 5.

Example of the response of the SSC to a PD pulse propagating into the stator winding from the end region of the winding, i.e. A triggers before B. Designation of traces as in Figure 3.

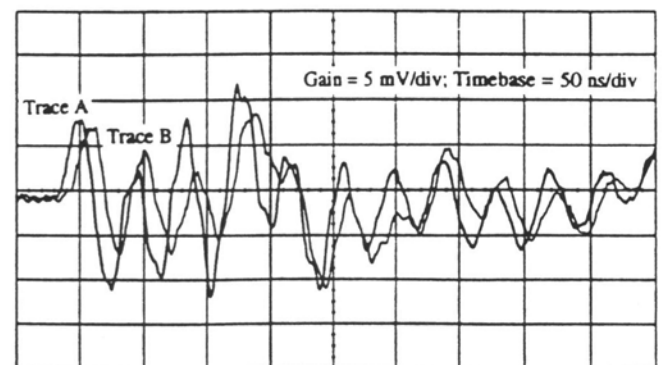


Figure 6.

Typical response of the SSC to electrical noise. Note the lower frequency characteristics of the noise response. Designation of traces as in Figure 3.

can have many characteristics in common with test piece PD, such as frequency content, ac phase position, repetition rate, etc. (Radio frequency signals from radio transmitters or power line carrier transmission are of less importance since they can be easily filtered out.) Such noise pulses can be mis-identified as legitimate PD pulses, which can lead to HV equipment incorrectly being identified as defective.

At present, skilled observers subjectively distinguish between noise and PD from the signals displayed on an oscilloscope screen. The distinguishing features depend on the application, but pulse position (with respect to the ac phase), magnitude, distribution of magnitudes, repetition rate, pulse duration and pulse pattern constancy are often used [19]. As discussed above, the introduction of post-detection processing makes this noise reduction less subjective. However even post-detection analysis cannot be absolute in rejecting many common types of noise pulses, and in particular PD and corona external to the test piece. This is because many of the characteristics of the noise are the same, or very similar, to the actual PD in the test piece. Also, PD in the test piece may have enough deviations from ideal PD pulses to exhibit characteristics of noise. An alternative means of reducing the influence of noise is to use a Kreuger bridge measuring system [1]. This is often effective, but cannot always be applied in field situations, for example where the test piece is grounded. In addition, it is difficult to balance the bridge to reduce the noise by more than about 10 x.

UWB detection, under certain circumstances, can provide a more certain means of noise rejection than the above-mentioned methods. UWB detection of pulses facilitates noise rejection by permitting the measurement of the direction of pulse propagation and/or pulse travel time. If a suitably designed PD detector is close to a PD source in the test piece, and another PD detector is nearer to the noise sources, then a pulse arriving at a detector closer to the test piece should be detected first.

Clearly for such a method to work, the PD detector must be able to respond to the ns PD pulses to distinguish the difference in arrival times. Therefore UWB detection can lead to certain noise elimination on a pulse-by-pulse basis, rather than by depending on a statistical elimination of noise based on macroscopic pulse pattern properties. Two examples of external noise rejection techniques, illustrating the above principles, are presented later.

2.3 IMPROVED UNDERSTANDING OF THE PD PROCESS

A final advantage of UWB detection is the ability to observe directly the shape of individual PD pulses. Observation of the true PD current pulse shape from a wide variety of PD sources has shown that there are differences in the pulse shape from different sources [18]. By comparing PD pulses from unknown sources with PD pulse shapes from

known sources, the nature of the PD in the test piece can be determined with more assurance. This is of practical importance since some types of PD are more dangerous to the integrity of the solid insulation than others. For example, in rotating machines it would be valuable to be able to differentiate between potentially damaging slot discharges and relatively benign transverse surface discharges in the endwinding. Furthermore, the ability to measure faithfully the current pulse shapes can aid in elucidating the PD process because UWB methods are able to resolve events on a time scale comparable with electronic transit times in a void.

To derive maximum benefit from PD measurements as discussed above, considerable research on the development of practical UWB PD detection systems has been undertaken. In some cases, particularly where on-line PD detection was essential to reduce outage time, a near perfect means of eliminating noise (to eliminate false alarms) was the motivator for using UWB PD detection. For other applications in relatively noise free environments, the greater sensitivity to sub-pC PD and the ability to determine PD pulse shape were the objectives.

3. ROTATING MACHINE APPLICATIONS

Partial discharge testing of the stator winding insulation systems of rotating machines has proved to be a valuable tool to aid in the assessment of insulation condition. Experience in this area has been predominantly with off-line testing. This type of testing is normally performed when the machine is removed from service for maintenance or repair. In the context of other diagnostic measurements and visual inspections, such off-line PD data can support the diagnosis of insulation condition. Partial discharge testing has proven effective in detecting problems such as (1) internal delamination in the groundwall insulation, and (2) deterioration of stress control systems.

Unfortunately, off-line testing is relatively ineffective in reliably detecting problems associated with the slot support system and with the endwinding. This **is because**, unlike during **normal operating conditions**, **there are no** magnetic forces present to cause movement of the stator bars/coils within the slot. Hence an off-line test will not necessarily detect slot discharge due to loose wedges. Another drawback is that under operating conditions, the voltage distribution in the winding is not normally simulated by an off-line test. Consequently, discharge phenomena related to problems in the endwinding are not usually manifest. In addition, implicit in the off-line test is the need for an outage and a 'PD free' HV power supply. Both requirements represent significant inconvenience and expense. Thus there is a demonstrable need for a reliable on-line PD test which would permit detection of PD under normal operating conditions, obviating the problems inherent in off-line testing.

However, a major difficulty associated with performing on-line PD monitoring is interference due to electrical noise.

The principal motivation for using high-frequency detection techniques is to improve signal-to-noise ratio thus permitting the possibility of high reliability on-line PD measurements. First, the major sources of generating station environment are discussed. The principal sources of electrical noise which hinder reliable on-line PD monitoring are (1) the excitation system, (2) shaft grounding schemes, (3) the isolated phase bus (IPB), (4) connected equipment, *e.g.* the generator transformer, and (5) arc welding equipment.

The synchronous nature of the excitation system noise renders this source amenable to synchronous noise rejection schemes. For example, pulse counting circuits can be inhibited for the duration of the pulses associated with the excitation system. Such schemes have been implemented previously [20]. The other interference sources listed above tend to be more problematic since they are essentially asynchronous and random in nature. Despite these difficulties, efforts have been made to implement on-line PD monitoring in hydraulic and turbine generators. Primarily, these techniques are based on either temporarily installing capacitive couplers at the phase terminals [13], or permanent installation of a high frequency current transformer (CT) at the generator neutral [21]. However, each of these techniques requires considerable skill and experience on the part of the operator to separate the component of the signal which is due to the PD from noise pulses. As discussed above, it is this subjective categorization of PD and noise which modern post-processing techniques seek to eliminate. However, the application of even the most sophisticated signal processing techniques does not necessarily render the measurement completely objective. This is because, inherent in these techniques, there still remains a subjective assessment as to what constitutes PD. A different approach to the problem is to make the differentiation of PD from noise an intrinsic property of the coupling device. For this reason, couplers with UWB capabilities are an attractive option. Two different methods of achieving high signal-to-noise ratio performance, by means of very high frequency couplers are discussed below.

3.1 HIGH FREQUENCY TECHNIQUES APPLIED TO HYDRAULIC GENERATORS

In this technique, known as the partial discharge analyzer (PDA) test, pairs of ‘balanced’ 80 pF coupling capacitors are permanently installed in a hydraulic generator stator winding [13] to detect PD and other high frequency electrical pulses. The PDA instrument takes the signals from a pair of couplers, subtracts the common mode noise in a method to be explained below, and sorts the remaining PD pulses by magnitude and number.

A minimum of two couplers, with capacitances differing by no more than ~ 2%, are installed on each phase of a line end coil of a parallel to the circuit ring bus. The lengths of the coaxial cables connecting the couplers from two

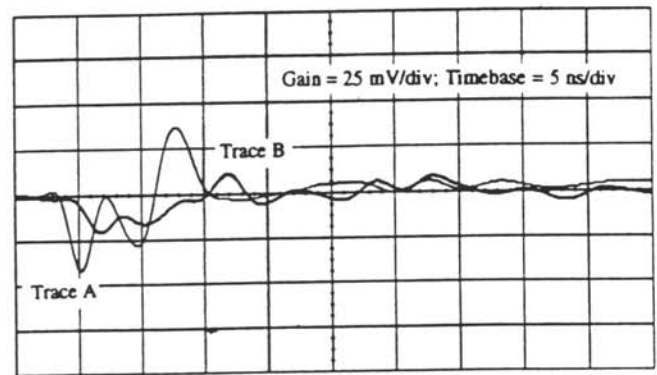


Figure 7.

Example of the attenuation of the high frequency component of a PD pulse propagating in a stator bar. Trace A and trace B refer to the outputs of two SSC units which are displaced by 30 cm from one another. Trace A is from the output of the SSC which is closest to the PD source. The high frequency component of the PD pulse is attenuated by 50% within 30 cm.

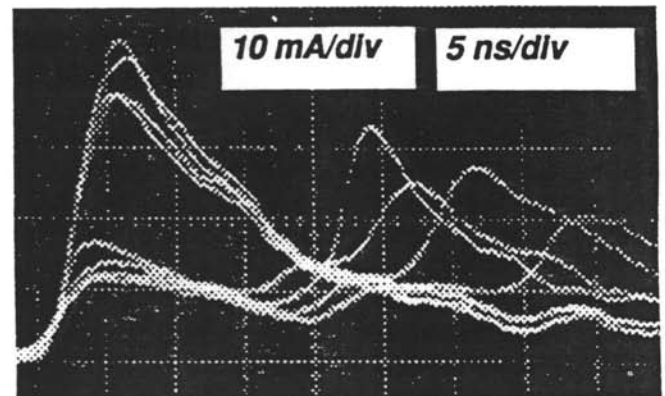


Figure 8.

Multiple exposure oscillogram showing an example of slow PD pulse shapes. Pulses of this type usually have varying shapes but usually have durations in the 10 to 20 ns range. The measurement was made with an oscilloscope with an analog bandwidth of 1000 MHz.

parallels in the same phase to the instrument terminal box external to the machine are adjusted so that the electrical length of the paths, from the machine terminal along the circuit ring bus to the terminal box, is the same within 0.5 m (1.5 ns) for the two couplers. This connection scheme is illustrated in Figure 2. Noise pulses external to the generator propagate along the circuit ring bus and are detected by the pair of couplers at the same time. Thus pulses from the two couplers arrive together at the differential input in the PDA instrument, and essentially cancel, whereas PD pulses from sites within the winding arrive at the instrument far enough separated in time to be recognized. In actual practice, the signal-to-noise ratio is often improved by the attenuation of external noise by ‘mismatching’ at the machine terminals. Also, some internal noise, such as static exciter transients, is effectively suppressed by the differential PDA input

because it is primarily in a relatively low frequency region where the difference in signal path lengths is insignificant. The Important point to note in the above description of this technique is that noise rejection is only rendered possible because of the wideband frequency response of the coupling devices. A PD pulse near one coupler results in a near immediate pulse which lasts a few ns in this coupler, whereas the far coupler does not respond to this pulse for the time it takes to propagate along the circuit ring bus, typically 30 ns. This difference in arrival time is readily distinguished with a high frequency differential amplifier. If the coupling system had a risetime in the order of 500 ns, the difference in the signals from the two couplers, time shifted by 30 ns, cannot be distinguished and no output would result from the differential amplifier. The PDA coupling system is installed on over 500 generators worldwide, and has proved the usefulness of UWB detection to reduce noise.

3.2 ULTRAWIDEBAND TECHNIQUES APPLIED TO TURBINE GENERATORS

Unfortunately the PDA technique cannot be transferred directly for application in turbine generators. This is due to two principal reasons. First, in general, the noise background levels in turbine generator stations can be up to 1000 x greater than the PD signal level. The PDA noise rejection technique used in hydraulic generators has only the ability to reduce noise by a factor of ten. A further problem is that the circuit ring bus in a turbine generator does not readily permit noise rejection using time of flight techniques. This is because the circuit ring bus on a turbine generator is normally a very compact structure, consequently the transit time of the pulses is too short to enable the technique to work. Thus a significantly different approach, using frequencies an order of magnitude higher than the PDA technique, has recently been introduced.

Efforts have been directed towards developing a wide bandwidth coupler which is capable of preserving the information inherent in a true representation of the temporal characteristics of a PD pulse. A coupling device which has the capability of performing these functions has recently been developed. This detector is known as wide bandwidth directional electromagnetic coupler which, as its name implies, is designed to be installed in the slot portion of the stator core. Specifically, the SSC is designed to be an integral component of the depth packing system in the slot. A more detailed description of the SSC can be found elsewhere [22]. The SSC has a bandwidth which extends from 10 MHz to > 1 GHz. This property permits observation of the true temporal response of the PD and the noise. Location of the SSC in the stator slot enhances its sensitivity to PD originating in the machine because of the well known severe attenuation of high frequency signals as they propagate in stator windings [23]. Using these two properties of the device, it is possible to distinguish between PD and noise because, although both

are detected by the SSC, each has a significantly different frequency content. That is, PD pulses are manifest as very fast temporal phenomena whereas, because the noise has to propagate some distance to reach the coupler, only the lower frequency components remain. This property of the SSC will be further illustrated and discussed below. In this case, we are taking advantage of the low pass filter characteristic of the stator structure. In addition the wide bandwidth response of the coupler may permit differentiation between noise and different types of PD phenomena by examination of the pulse shapes. Experimental evidence which illustrates this point exists, and results will be discussed in the Section on GIS. Similar experimental work for rotating machines has yet to be performed.

At present, SSC has been installed on eight turbine generators rated > 300 MW. Examples of PD obtained from an operating 22 kV, 500 MW turbine generator are illustrated in Figure 3. These traces were recorded on a Tektronix 7104 analog oscilloscope with a bandwidth of 900 MHz. Features to note in the Figures are the risetime (≈ 2 ns) and the total pulse duration, of the order of 5 to 10 ns. These Figures illustrate that fast PD phenomena, as discussed in the Introduction, can be detected in lossy systems such as stator windings, as well as in more 'ideal' systems such as GIS. Figure 4, recorded on a Hewlett-Packard (HP) 54111D digitizing oscilloscope, with a single shot bandwidth of 250 MHz, and a sampling rate of 1 GSa/s, also illustrates a PD pulse detected on an operating 22 kV, 500 MW machine.

Another feature to note in Figure 4 is the two port design of the SSC. Trace A is the response of the SSC output which is located within a few cm of the end of the stator core. Trace B is the response at the second output of the SSC which is located 45 cm further into the slot portion of the core. Hence the traces illustrated in Figure 4 represent a PD pulse propagating outward from the slot portion of the stator winding. Using similar arguments, and the same designation of traces as above, Figure 5 illustrates a PD pulse propagating into the stator winding. Figures 4 and 5 demonstrate the ability of the SSC to detect the high frequency components of PD occurring within the machine. In contrast Figure 6 shows the responses due to the SSC, recorded on the HP 54111D, which result from electrical noise. The basic differences between Figure 4, representing a PD pulse, and Figure 6, illustrating a noise pulse, are the rise time and pulse duration. Electrical noise can be characterized by a relatively slow rise time, of 15 to 20 ns, and a low frequency oscillation with a duration of $\sim 1/\text{ms}$. These responses have been replicated on each of the generator on which measurements of SSC response have been made. Additional verification was provided by installing an SSC on a neutral bar, where the probability of PD is extremely low. Fast pulse phenomena were not observed from SSC located at these points. Experiments on operating generators also show that the slow responses all propagate into the winding, indicative of external influences

coupling into the stator via the IPB.

The rationale for defining phenomena, such as displayed in Figure 4 as PD and Figure 6 as noise, is as follows. Previous work has shown that high frequency signals are heavily attenuated in stator windings [23,24]. However, the SSC is located as close as possible to the line end of the stator winding, i.e. close to the PD source of interest. Consequently, the SSC is ideally located to detect the high frequency component of the PD. Experiments on PD pulse propagation on a 500 MW stator winding, Figure 7, indicate that the high frequency components of the pulse to two principal reasons. First, in general, the noise background levels in turbine generator stations can be up to 1000 x greater than the PD signal level. The PDA noise rejection technique used in hydraulic generators has only the ability to reduce noise by a factor of ten. A further problem is that the circuit ring bus in a turbine generator does not readily permit noise rejection using time of flight techniques. This is because the circuit ring bus on a turbine generator is normally a very compact structure, consequently the transit time of the pulses is too short to enable the technique to work. Thus a significantly different approach, using frequencies an order of magnitude higher than the PDA technique, has recently been introduced [22].

Efforts have been directed towards developing a wide bandwidth coupler which is capable of preserving the information inherent in a true representation of the temporal characteristics of a PD pulse. A coupling device which has the capability of performing these functions has recently been developed. This detector is known as the stator slot coupler (SSC). The SSC is a wide bandwidth directional electromagnetic coupler which, as its name implies, is designed to be installed in the slot portion of the stator core. Specifically, the SSC is designed to be an integral component of the depth packing system in the slot. A more detailed description of the SSC can be found elsewhere [22]. The SSC has a bandwidth which extends from 10 MHz to > 1 GHz. This property permits observation of the true temporal response of the PD and the noise. Location of the SSC in the stator slot enhances its sensitivity to PD originating in the machine because of the well known severe attenuation of high frequency signals as they propagate in stator windings [23]. Using these two properties of the device, it is possible to distinguish between PD and noise because, although both are detected by the SSC, each has a significantly different frequency content. That is, PD pulses are manifest as very fast temporal phenomena whereas, because the noise has to propagate some distance to reach the coupler, only the lower frequency components remain. This property of the SSC will be further illustrated and discussed below. In this case, we are taking advantage of the low pass filter characteristic of the stator structure. In addition the wide bandwidth response of the coupler may permit differentiation between noise and different types of PD phenomena by examination of the

pulse shapes. Experimental evidence which illustrates this point exists, and results will be discussed in the Section on GIS. Similar experimental work for rotating machines has yet to be performed.

At present, SSC has been installed on eight turbine generators rated > 300 MW. Examples of PD obtained from an operating 22 kV, 500 MW turbine generator are illustrated in Figure 3. These traces were recorded on a Tektronix 7104 analog oscilloscope with a bandwidth of 900 MHz. Features to note in the Figures are the risetime [≈ 2 ns] and the total pulse duration, of the order of 5 to 10 ns. These Figures illustrate that fast PD phenomena, as discussed in the Introduction, can be detected in lossy systems such as stator windings, as well as in more 'ideal' systems such as GIS. Figure 4, recorded on a Hewlett-Packard (HP) 54111D digitizing oscilloscope, with a single shot bandwidth of 250 MHz, and a sampling rate of 1 GSa/s, also illustrates a PD pulse detected on an operating 22 kV, 500 MW machine.

Another feature to note in Figure 4 is the two port design of the SSC. Trace A is the response of the SSC output which is located within a few cm of the end of the stator core. Trace B is the response at the second output of the SSC which is located 45 cm further into the slot portion of the core. Hence the traces illustrated in Figure 4 represent a PD pulse propagating outward from the slot portion of the stator winding. Using similar arguments, and the same designation of traces as above, Figure 5 illustrates a PD pulse propagating into the stator winding. Figures 4 and 5 demonstrate the ability of the SSC to detect the high frequency components of PD occurring within the machine. In contrast Figure 6 shows the responses due to the SSC, recorded on the HP 54111D, which result from electrical noise. The basic differences between Figure 4, representing a PD pulse, and Figure 6, illustrating a noise pulse, are the rise time and pulse duration. Electrical noise can be characterized by a relatively slow rise time, of % 15 to 20 ns, and a low frequency oscillation with a duration of $\sim 1/\mu$ s. These responses have been replicated on each of the generators on which measurements of SSC response have been made. Additional verification was provided by installing an SSC on a neutral bar, where the probability of PD is extremely low. Fast pulse phenomena were not observed from SSC located at these points. Experiments on operating generators also show that the slow responses all propagate into the winding, indicative of external influences coupling into the stator via the IPB.

The rationale for defining phenomena, such as displayed in Figure 4 as PD and Figure 6 as noise, is as follows. Previous work has shown that high frequency signals are heavily attenuated in stator windings [23,24]. However, the SSC is located as close as possible to the line end of the stator winding, i.e. close to the PD source of interest. Consequently, the SSC is ideally located to detect the high frequency component of the PD. Experiments on PD pulse propagation on a 500 MW stator winding, Figure 7, indicate

that the high frequency components of the pulse PD usually occurs at much lower rates, measurements are accumulated for a period of 5s. The data collected are downloaded to a host computer which processes and displays the data in an appropriate form.

4.3 PD MEASUREMENT RESULTS

PD pulse waveshapes in GIS are generally known to have fast risetimes and short durations [16]. However, UWB measurements permit accurate recordings of PD pulse shape and have indicated the existence of at least two distinct categories of PD pulses. The first is the classic fast, narrow pulse with sub-ns to ns risetimes and ns durations as discussed above. The second type of PD pulse has a much broader shape (10 to 20 ns pulse width) and longer risetimes (several ns) and usually (but not always) a lower magnitude. Typical PD pulse shapes of these two categories are shown in Figures 1 and 8. In addition, in many cases, PD pulse shapes suggest composite pulses possibly indicative of multiple discharge events within the void volume.

Many of the over 300 GIS insulators, tested at 400 kV with this system, exhibited both types of PD pulse shapes whereas some exhibited only one type of PD pulse. With the present measurement apparatus, the existence of a causal link between the two types of pulses and specific discharge processes cannot be determined. However, other observations indicate that one type of pulse may 'trigger' the occurrence of other types of pulses. The two distinct pulse shapes indicate that at least two different discharge mechanisms are possible within voids. The physical mechanisms are complex and probably related to the dynamics of charge movement and distribution on the void wall. In this manner, the discharge mechanism(s) is probably related to the material properties which affect the characteristics of the void wall, including epoxy formulation, filler type, void wall topography and void formation (void size and gas composition), and void surface conductivity. Preliminary, simultaneous optical/electrical measurements of void discharges in laboratory samples with clear, unfilled epoxy samples suggested that the fast, narrow PD pulses correspond to 'streamer-like' discharges within the void gas or along the void wall surface, whereas the slower PD pulses correspond to more diffuse discharges apparently involving most of the void volume [28]. The existence of two types of pulses has possible implications on the degradation mechanisms associated with PD in voids. Once these phenomena are better understood, there may be a need as well to discriminate between the two types of pulses in assessing acceptable PD levels.

The post-processed display of accumulated counts of PD pulses resolved by polarity, magnitude (pulse height) and phase of the applied ac voltage has also revealed distinct patterns or 'signatures' whose specific features may correspond to fundamental discharge processes. However, the measured patterns are often unstable and change as

a function of time and voltage (as do void wall surface characteristics) making it difficult to correlate them with other observations [29]. Further investigations are required to precisely determine the significance of these patterns.

Some of the common features in the phase-resolved patterns which are frequently observed for insulators with void defects are illustrated in Figures 9 and 10. The pattern of Figure 9 is the 'classic' PD pattern of roughly equal populations of positive and negative counts which is often observed for many types of defects over a wide range of voltages. Figure 10 shows a measurement with the unique feature of a curved pattern which can be seen easily in the Figure, but is not evident on the pulse height analysis. This sample also shows two distinct populations of PD counts, the second of which appears similar to that of Figure 9. However, the curved feature has on occasion been observed in isolation. In addition, the two components of the pattern will sometimes appear to merge and blend into each other whereas in other cases, the two components are extremely distinct. These developments, in most cases, appear to be voltage and time dependent. Possible physical processes which might give rise to such a pattern are not immediately obvious but are presently under investigation.

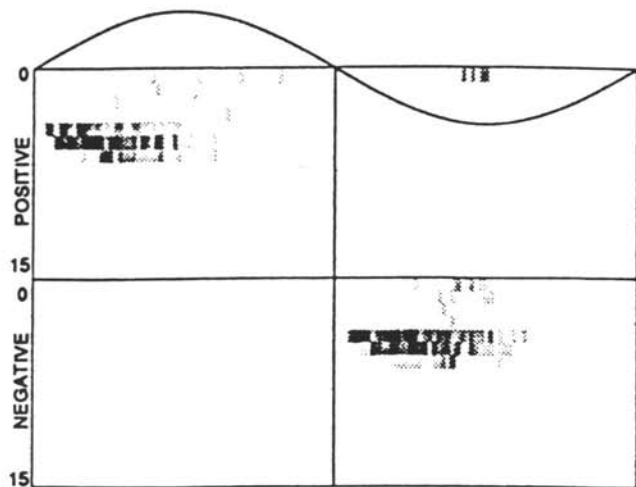
Preliminary analysis of void PD indicates that patterns such as the curved one indicated in Figure 10 are more readily apparent if the data, collected with UWB detection, are displayed in terms of pulse height (peak PD pulse current) as opposed to integrated charge, as would be the case for conventional detection. In one particular case, a phase-resolved plot of the pulse height clearly indicated the same curved pattern of Figure 10, whereas the plot of the same data as integral charge resulted in a less informative 'cluster' pattern, similar to that of Figure 9 [28].

The fast, narrow PD pulses (high pulse height/integral charge ratio) seem to correspond to a type of discharge which might be more damaging in terms of insulation degradation (as a result of higher energy densities in the discharge plasma) as compared to the more diffuse discharge associated with the slower PD pulses (lower pulse height/integral charge ratio). However, in cases where both types of pulses occur, measurement of the pulse height, which is only possible using UWB detection, is

5. CONCLUSIONS

THIS work has shown that significant improvements in PD measurement can be achieved through the use of UWB coupling techniques. These enhancements are principally in the areas of increased sensitivity, external noise rejection, and better understanding of the physics of the PD process. Examples of the improvements achievable by the use of UWB techniques were discussed for the cases of rotating machines and GIS.

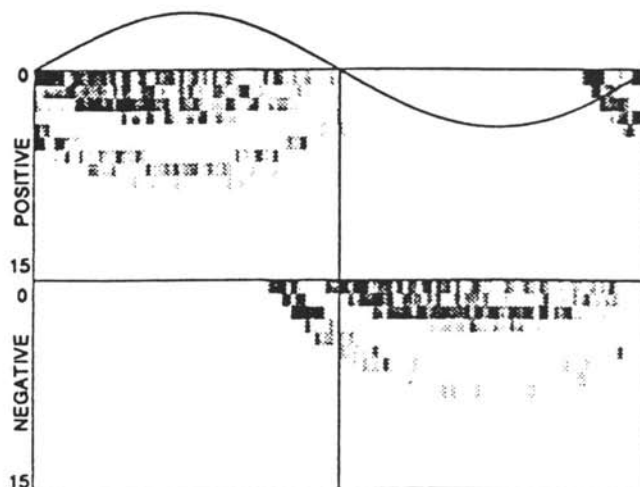
A new PD coupler, known as the SSC, which has a frequency response extending into the GHz range, was demonstrated to



CHA	(COUNTS)		mV	pC
	POS	NEG		
0	12	9	0.3	0.02
1	1	4	0.5	0.03
2	2	1	0.8	0.05
3	1	1	1.3	0.08
4	62	148	2.0	0.13
5	195	126	3.2	0.21
6	32	15	5.0	0.32
7	0	0	7.9	0.52
8	0	0	12.6	0.82
9	0	0	19.9	1.29
10	0	0	31.5	2.05
11	0	0	50.0	3.25
12	0	0	79.2	5.15
13	0	0	125.6	8.16
14	0	0	199.1	12.94
15	0	0	315.5	20.51
TOT	305	304		

Figure 9.

Example of commonly observed PD measurement pattern of a void discharge in an epoxy insulator. Data are displayed resolved by pulse polarity, magnitude (16 channels, logarithmically spaced for each polarity) and phase of the applied voltage. The number of accumulated PD counts (over a 5 s interval) is indicated by the grey tone of the Figure. A simple pulse height analysis is also shown with corresponding mV and pC levels. The pC level is an integrated value based on a typical (fast type) pulse shape.



CHA	(COUNTS)		mV	pC
	POS	NEG		
0	339	247	0.2	0.01
1	177	190	0.3	0.02
2	238	268	0.4	0.03
3	63	32	0.6	0.04
4	23	13	1.0	0.06
5	32	9	1.6	0.10
6	36	13	2.5	0.16
7	34	3	4.0	0.26
8	5	4	6.3	0.41
9	0	0	10.0	0.65
10	0	0	15.8	1.03
11	0	0	25.1	1.63
12	0	0	39.7	2.58
13	0	0	62.9	4.09
14	0	0	99.8	6.48
15	0	0	158.1	10.28
TOT	947	799		

Figure 10.

Example of a commonly observed PD measurement pattern (phase-resolved and pulse-height plots) showing a well-defined curved pattern in addition to a second population of counts. These characteristics have been observed for PD from voids in insulators.

enable reliable discrimination of PD signals from noise on operating turbine generators. Results were presented which clearly show the different temporal characteristics of PD and noise signals.

A measurement sensitivity of 0.01 pC was achieved, primarily through the use of UWB techniques, in a system designed to perform quality control testing of insulating spacers for GIS application. In addition, preliminary results from a fundamental study on PD in epoxy resins, showed that there are two types of PD phenomena, i.e. 'fast' and 'slow'. The 'fast' PD may be associated with 'streamer' type discharges whereas the slower PD pulses correspond to diffuse discharges apparently involving most of the void volume.

REFERENCES

- [1] R. Bartnikas, and E. J. McMahon, "Engineering Dielectrics. Corona Measurement and Interpretation", Vol. 1, STP 669, ASTM, Philadelphia, 1979.
- [2] R. Bartnikas, "Nature of Partial Discharges and Their Measurement", Annual Report, Conference Electrical Insulation and Dielectric Phenomena, Gaithersburg, Md. 1987, 87 CH2462-0, pp. 13-44, 1987.
- [3] R. Bartnikas, and J. H. Levi, "A Simple Pulse Height Analyzer for Partial Discharge Rate Measurements", IEEE Transactions on Instrumentation and Measurement, Vol. 18, pp. 403-407, 1969.
- [4] A. Kelen, "The Functional Testing of HV Generator Stator Insulation", CIGRE Paper 15-03, 1976.

- [5] H. Matsuzaki, T. Ito, Y. Ehara, T. Sakai, P. J. McKenny, and M. Hammam, "Internal Discharge Pulse Measurement Using a Microcomputer", Annual Report, Conference on Electrical Insulation and Dielectric Phenomena, Claymont Del, 86CH2315-0, pp. 438-443, 1986.
- [6] Y. J. Kirn, and J. K. Nelson, "A New Parameter for the Prediction of Deterioration in Epoxy Groundwall Insulation", Annual Report, Conference on Electrical Insulation and Dielectric Phenomena, Ottawa Canada, 88CH2668-2, pp. 122-127, 1988.
- [7] J. L. Tripier, P. Maurin, and D. Lefevre, "New Trends in Interpretation of Partial Discharge Measurements", Conference Record of the 1990 Int. Symposium on Electrical Insulation, Toronto Canada 1990, 90CH2727-6, pp. 111-114, 1990.
- [8] B. Fruth, and J. Fuhr, "Partial Discharge Pattern Recognition - A Tool for Diagnosis and Monitoring of Aging", CIGRE Paper 15/33-12, 1990.
- [9] M. Kahle, E. Neudert, J. Herrman, O. Schneider, and R. Roding, "Progress in the Field of PD Monitoring of Aging Processes of HV Insulation", CIGRE Paper 15/33-13, 1990.
- [10] Y. Ehara, T. Saito, M. Matsudo, T. Ito, K. Jogan, and M. Hammam, "Correlation Between Discharge Magnitude Distribution and Discharge Luminescence Due to Electrical Treeing", Annual Report, Conference on Electrical Insulation and Dielectric Phenomena, Pocono Manor Pa, 90CH2919-9, pp. 313-318, 1990.
- [11] J. M. Braun, S. Rizzetto, N. Fujimoto, K. J. Diederich, and A. Girodet, "Behavior of GIS Epoxy Insulators with Metallic Inclusions", Annual Report, Conference on Electrical Insulation and Dielectric Phenomena, Pocono Manor Pa, 90CH2919-9, pp. 425-432, 1990.
- [12] M. Pompili, C. Mazzetti, and R. Schifani, "Partial Discharge Amplitude Distribution of Power Transformer Oils", Symposium on Electrical Insulation, Toronto Canada, 90 CH2727-6, pp. 133-136, 1990.
- [13] M. Kurtz, J. F. Lyies, and G. C. Stone, "Application of Partial Discharge Testing to Hydrogenerator Maintenance", IEEE Transactions on Power Apparatus and Systems, Vol. 103, 1984, pp. 2148-2157.
- [14] M. Kurtz, and G. C. Stone, "Diagnostic Testing of Generator Insulation, Part II - An Improved Partial Discharge Test", Canadian Electrical Association Research Report, RP76-17, 1978.
- [15] T. Okamoto, and T. Tanaka, "Novel Partial Discharge Measurement Computer-Aided Systems", IEEE Transactions on Electrical Insulation, Vol. 21, pp. 1015-1019, 1986.
- [16] S. A. Boggs, and G. C. Stone, "Fundamental Limitations in the Measurement of Corona and Partial Discharge", IEEE Transactions on Electrical Insulation, Vol. 17, pp. 143-150, 1982.
- [17] B. Luczynski, Partial Discharges in Artificial Gas Filled Cavities in Solid HV Insulation, PhD Thesis, Technical University of Denmark, 1979.
- [18] G. C. Stone, and S. A. Boggs, "Wide Band Measurements of Partial Discharge in Epoxy", Int. Symposium on Electrical Insulation, Philadelphia, Pa, 82CH1773-1, pp. 137-140, 1982.
- [19] CIGRE Study Group 21.03, "Recognition of Discharges", *Electra*, Vol. 11, pp. 61-98, 1969.
- [20] M. Kurtz, and G. C. Stone, "Diagnostic Testing of Generator Insulation, Part III - The Partial Discharge Analyzer and Coupling Systems", Canadian Electrical Association Research Report, RP76-17, 1980.
- [21] F. T. Emery, and R. T. Harrold, "On-line Incipient Arc Detection in Large Turbine Generator Stator Windings", IEEE Transactions on Power Apparatus and Systems, Vol. 99, pp. 2232-2240, 1980.
- [22] H. G. Sedding, S. R. Campbell, G. C. Stone and G. S. Klempner, "A New Sensor for Detecting Partial Discharge in Operating Turbine Generators", 1991 IEEE Winter Power Meeting, New York NY, Paper 91 WM 065-3-EC, 1991.
- [23] M. Henriksen, G. C. Stone, and M. Kurtz, "Propagation of Partial Discharge and Noise Pulses in Turbine Generators", IEEE Transactions on Energy Conversion, Vol. 1, pp. 161-166, 1986.
- [24] A. Wilson, R. J. Jackson, and N. Wang, "Discharge Detection Techniques for Stator Windings", *Proc. IEE*, Vol. 132 B, pp. 234-244, 1985.
- [25] S. A. Boggs, "Electromagnetic Techniques for Fault and Partial Discharge Location in Gas Insulated Cables and Substations" IEEE Transactions on Power Apparatus and Systems, Vol. 101, pp. 1935-1941, 1982.
- [26] D. Lightle, B. Hampton and T. Irwin, "Monitoring of GIS at Ultra High Frequency", *Proc. Sixth Int. Symposium on HV Engineering*, New Orleans, La., Paper 23.02, 1989.
- [27] S. Rizzetto, N. Fujimoto and G. C. Stone, "A System for the Detection and Location of Partial Discharges Using X-rays", Int. Symposium on Electrical Insulation, Boston MA, 88CH2594-0-DEI, pp. 262-266, 1988.
- [28] J. T. Holboll, J. M. Braun, N. Fujimoto and G. C. Stone, "Discharge Phenomena in Voids in Epoxy: Simultaneous Detection of Optical and Electrical Signals", Submitted to the 7th Int. Symposium on High Voltage Engineering, Dresden Germany, 1991.
- [29] N. Fujimoto, "Characteristics of Ultra-low Level Partial Discharges in GIS Epoxy Insulators", in *Gaseous Dielectrics VI*, L. G. Christophorou and I. Sauers Eds, Plenum Press NY, pp. 509-516, 1991.

1. now with IRIS Power Engineering Inc., Mississauga, Ontario, Canada.

Manuscript was received on 17 January 1991, in Snal form 21 Jan 1992.